

## Metallogenic Fluid Characteristics of Yueshan Cu-polymetallic Deposit

Chenguang Zhang<sup>1,2\*</sup>, Haifeng Hu<sup>3</sup>, Daohan Zha<sup>4</sup>, Haidong Jiang<sup>5</sup>

<sup>1</sup> College of Geographic Science, Henan Key Laboratory for Synergistic Prevention of Water and Soil Environmental Pollution, Southern Henan Center for Mineral Rock and Gem-Jade Identification and Processing, Xinyang Normal University, Xinyang 464000, China

<sup>2</sup> Key Laboratory of Metallogenic Prediction of Nonferrous Metals and Geological Environment Monitoring (Central South University), Ministry of Education, Changsha 410083, China

<sup>3</sup> Hunan Geology Exploration Institute of China Chemical Geology and Mine Bureau, Changsha 410004, China

<sup>4</sup> Hunan Key Laboratory of Land Resources Evaluation and Utilization, Changsha 410007, China

<sup>5</sup> Institute of Resources and Environmental Engineering, Guizhou University of Technology, Guiyang 550003, China

Corresponding Author Email: [paladin@xynu.edu.cn](mailto:paladin@xynu.edu.cn)

<https://doi.org/10.18280/ijht.370217>

### ABSTRACT

**Received:** 12 January 2019

**Accepted:** 12 March 2019

**Keywords:**

*fluid inclusion, hydrotogenesis, fluid, temperature*

Yueshan Cu-polymetallic deposit Located between the Yangtze Plate, the Qinling–Dabie orogenic belt and is characterized by excellent metallogenic conditions. This paper attempts to disclose the hydrotogenesis mechanism of Yueshan Cu-polymetallic deposit. The metallogenic mechanism of material and fluid sources under the action of heat sources was discussed through fluid inclusion analysis. In this way, the physical-chemical conditions and fluid composition of hydrotogenesis were determined, revealing the fluid and temperature features of hydrotogenesis. It is concluded that the metallogenic fluid of Yueshan Cu-polymetallic deposit belongs to the type of Na<sup>+</sup>+Ca<sup>2+</sup>+K<sup>+</sup>+Mg<sup>+</sup>+Cl<sup>-</sup>(SO<sub>4</sub><sup>2-</sup>), and the hot magma fluid was mineralized under 450–521 °C. Yanshanian magmatic intrusion provided heat source for metallogenic hydrothermal fluid of Yueshan Cu-polymetallic deposit. The fluid activity underwent skarn hydrothermal stage and tectonic hydrothermal stage, and the skarn minerals formed in the early stage were superimposed and enriched.

## 1. INTRODUCTION

Located between the Yangtze Plate, the Qinling–Dabie orogenic belt, and the North China Plate, the polymetallogenic belt (copper-iron-gold) in the middle and lower reaches of the Yangtze River is the most important metallogenic belt in eastern China. There are many mining areas in this metallogenic belt. One of them is Yueshan Cu-polymetallic deposit, which lies close to the southern Anhui city of Anqing [1-5].

Many scholars have explored the basic geology, regional metallogenesis, rock genesis and metallogenic stage of Yueshan mine, yielding fruitful results. In addition, several universities and science institutes, namely, China University of Geoscience and Central South University, have discussed the metallogenic mechanism of Yueshan mine, considering the correlation of metallogenesis with magmatite, strata and geological structure. However, there is little report on the hydrotogenesis mechanism of Yueshan mine [6-8].

To make up for the gap, this paper carefully examines minerals collected from Yueshan mine, using optical microscope, Linkam THMSG600 geological hot and cold stage and Dionex DX-120 ion chromatograph. In this contribution, on the basis of identification of ore-forming stages, we investigated fluid sources, physicochemical conditions for mineralization of the Yueshan Cu-polymetallic deposit, combining fluid inclusion study with geological evidence and stable isotopic analysis.

## 2. METHODOLOGY

Ranging from garnet, diopside, quartz to calcite, minerals in different metallogenic stages were tested on Linkam THMSG600 geological hot and cold stage under the temperature of -196–600°C. The instrument precision is ±1°C under 10–600 °C and ±0.1°C under -196–0°C.

During the test, the hot and cold stage was used to measure the following indices of fluid inclusions: the freezing temperature, the initial ice melting temperature, the final ice melting temperature, homogenization temperature and daughter mineral melting temperature. Next, the salinity, density and homogenization pressure of the fluid were computed by the equation from, with the aid of the FLINCOR program [9-14].

### 2.1 Microphysiography of fluid inclusions

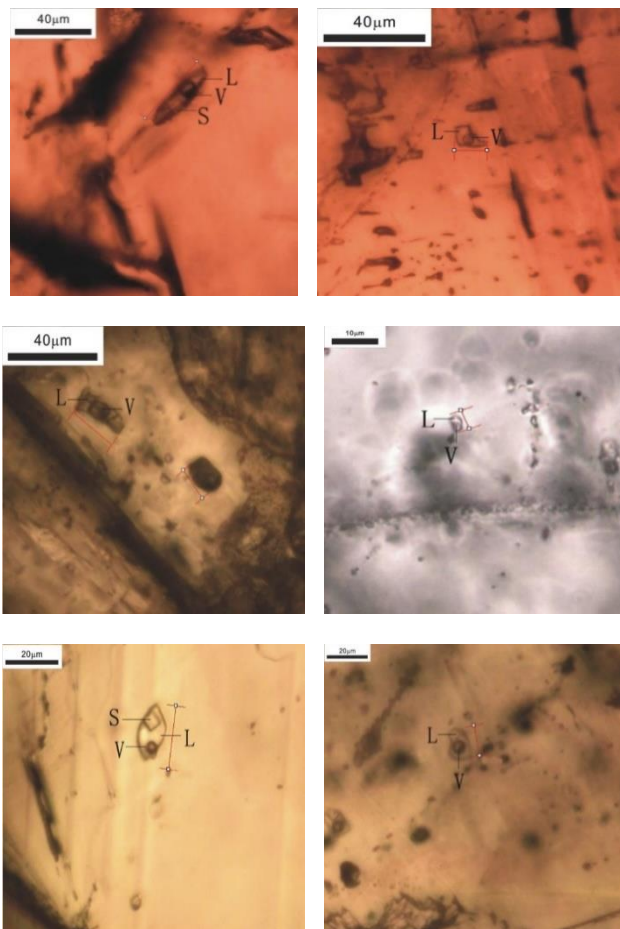
In Yueshan Cu-polymetallic deposit, the host minerals of fluid inclusions are garnet, diopside, quartz and calcite. Thus, the micro physiography of these minerals was studied in the samples collected from Yueshan Cu-polymetallic deposit. The micro physiographic features are listed in Table 1 below.

The fluid inclusions in the mine are either protogenetic or epigenetic. There are relatively few inclusions in the deposit, most of which are elliptical or irregular, falling between 6 and 19µm.

**Table 1.** The microphysiographic features of fluid inclusions

ID	Shape	Kind	Size	GLR
1	ellipse, rectangular, irregular - shaped	Ia, II	11 $\mu$ m - 52 $\mu$ m	15%-40%
2	ellipse, rectangular, irregular - shape	II	6 $\mu$ m - 19 $\mu$ m	15%-30%
3	ellipse, rectangular, irregular - shape	II	7 $\mu$ m - 11 $\mu$ m	15%-30%
4	ellipse, rectangular, irregular - shape	Ia, Ib, II	7 $\mu$ m - 32 $\mu$ m	15%-40%

At room temperature, the fluid inclusions in the deposit can be divided into halite crystal-containing multiphase inclusion (type I) and gas-liquid two-phase inclusion (type II), according to the composition, ratio and combination of different phases. Type I inclusions can be further split into two subtypes by the order of disappearance of halite crystal and bubble under heating: subtype Ia (halite crystal disappears first under heating) and subtype Ib (bubble disappears first under heating). The fluid inclusions observed in our study are all saline systems with little presence of CO<sub>2</sub>. The micrographs on different minerals in Yueshan Cu-polymetallic deposit are presented in Figure 1 below.

**Figure 1.** The micrographs on different minerals in Yueshan deposit

(a) Type I inclusions in garnet; (b) Type II inclusions in garnet;

(c) Type II inclusions in diopside; (d) Type II inclusions in quartz;

(e) Type I inclusions in calcite; (f) Type II inclusions in calcite.

As shown in Figure 1, type I inclusions were mainly developed in garnet and calcite. Most subtype Ia inclusions were protogenetic, and produced in garnet and calcite; Ranging between 10 and 30 $\mu$ m in size, subtype Ia inclusions were primarily elliptical or irregular and generated individually, with a gas-liquid ratio of 30~40%; the halite crystals of subtype Ia inclusions were cubic. Most subtype Ib inclusion were developed in calcite; Ranging between 8 and 30 $\mu$ m in size, subtype Ib inclusions were irregular in shape and generated individually, with a gas-liquid ratio of 20~35%; the halite crystals of subtype Ib inclusions were also cubic. Overall, subtypes Ia and Ib mainly differed in the inclusion morphology under heating, with no significant difference in shape or gas-liquid ratio.

As a common type of inclusions, type II inclusions were observed in garnet, diopside, quartz and calcite. Ranging between 7 and 30 $\mu$ m in size, most type II inclusions were elliptical, elongated or irregular, with a gas-liquid ratio of 15%~30%. In a few cases, the gas-liquid ratio could reach 40%.

## 2.2 Physical-chemical conditions of fluid inclusions

The fluid inclusions of garnet, diopside, quartz and calcite were subjected to temperature measurement by freezing and homogenization methods. The measured results are recorded in Table 2. The statistical histograms of homogenization temperature and salinity were plotted through statistical calculations (Figures 2 and 3). The physical-chemical conditions of fluid inclusions were detailed below.

### (1) Early skarn stage:

The fluid inclusions mainly existed in garnet and diopside. Most of the inclusions in garnet belonged to type II, and some belonged to type Ia.

Type II inclusions were all homogeneous to liquid phase at the temperature of 326~499 $^{\circ}$ C (mean: 443 $^{\circ}$ C); the final ice melting temperature was -19.7~-10.2 $^{\circ}$ C (mean: -14.6 $^{\circ}$ C), corresponding to the salinity of 14.2%~22.2%NaCleqv (mean: 18.0%NaCleqv) and density of 1.08~1.09 (mean: 0.69). Thus, the homogenization pressure was computed as 639~1,066bar.

For type Ia inclusions, the homogenization temperature was 465~521 $^{\circ}$ C (mean: 496 $^{\circ}$ C), corresponding to the salinity of 39.6%~42.3%NaCleqv (mean: 40.6%NaCleqv) and density of 1.08~1.09 (mean: 1.09). Thus, the homogenization pressure was computed as 1,120~1,593bar.

All inclusions in diopside belonged to type II, and were homogeneous to liquid phase at the temperature of 344~462 $^{\circ}$ C (mean: 324 $^{\circ}$ C); the final ice melting temperature was -14~-6.7 $^{\circ}$ C (mean: -10.22 $^{\circ}$ C), corresponding to the salinity of 10.10%~17.77%NaCleqv (mean: 13.97%NaCleqv) and density of 0.67~0.93 (mean: 0.84). Thus, the homogenization pressure was computed as 207~6,842bar.

### (2) Quartz sulfide stage

The fluid inclusions were mainly developed in quartz. All of them belongs to type II. During the test, type II inclusions were all homogeneous to liquid phase at the temperature of 298~406 $^{\circ}$ C (mean: 344 $^{\circ}$ C); the final ice melting temperature was -17.2~-8.9 $^{\circ}$ C (mean: -12.79 $^{\circ}$ C), corresponding to the salinity of 12.7%~20.4%NaCleqv (mean: 16.5%NaCleqv)

and density of 0.76~0.91 (mean: 0.84). Thus, the homogenization pressure was computed as 101~1,237bar.

(3) Carbonate stage

Calcite was the leading host mineral of fluid inclusions. Most inclusions belonged to type II, and some belonged to type I.

**Table 2.** Measured temperatures of the fluid inclusions in Yueshan mine

ID		580-1-9b	400-2-9	340-28-1	700-1-3b		
Host mineral fluid		Garnet		Diopside	Silica	Calcite	
		Ia	II	II	II	Ia	II
T (°C)	range		-56.1~-50.1	-51.3~-70.2	-68.2~-48.6		
	average		-53.24	-58.3	-58.34		
MT (°C)	range		-19.7~-10.2	-14~-6.7	-17.2~-8.9		
	average		-14.56	-10.22	-12.79		
DMT (°C)	range	319~349				273~340	265~285
	average	330				311	274
G-L-U-T (°C)	range	465~521	326~499	344~462	298~406	338~465	218~312
	average	495.8	443.3	394.2	343.9	402.3	266.6
salinity (%)	range	39.6~42.3	14.2~22.2	10.1~19.8	12.7~20.4	36.2~41.5	35.7~37.1
	average	40.6	18.0	14.5	16.5	39.1	36.2
density (g/cm <sup>3</sup> )	range	1.08~1.09	0.50~0.91	0.67~0.93	0.76~0.91	1.08~1.10	1.10~1.15
	average	1.09	0.69	0.84	0.84	1.09	1.11
Uniform pressure (MPa)	range	112~159	64~107	21~68	10~124	146~219	60~165
	average	142	76	45	75	174	90

All type II inclusions were homogeneous to liquid phase at the temperature of 3,266~499°C (mean: 443°C); the final ice melting temperature was -16.5~-9.8°C (mean: -14.3°C), corresponding to the salinity of 18.2%~19.8%NaCleqv (mean: 17.9%NaCleqv) and density of 0.95~0.96 (mean: 0.96). Thus, the homogenization pressure was computed as 451~559bar.

For type Ia inclusions, the homogenization temperature was 338~465°C (mean: 402.30°C), corresponding to the salinity of 36.2%~41.5%NaCleqv (mean: 39.1%NaCleqv) and density of 1.08~1.10 (mean: 1.09). Thus, the homogenization pressure was computed as 1,457~2,188bar.

For type Ib inclusions, the homogenization temperature was 218~312°C (mean: 267°C), corresponding to the salinity of 35.7%~37.1%NaCleqv (mean: 36.2%NaCleqv) and density of 1.08~1.09 (mean: 1.09). Thus, the homogenization pressure was computed as 601~1,654bar.

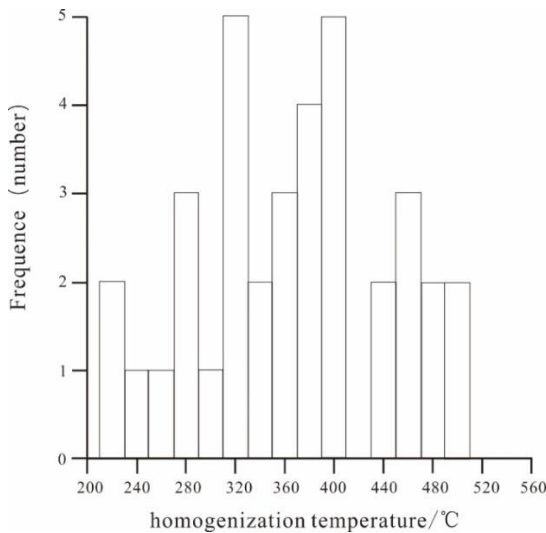


**Figure 2.** Statistical histogram of homogenization temperature of fluid inclusions

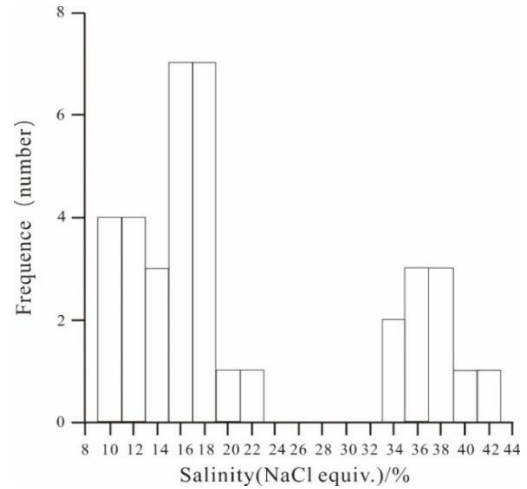


**Figure 3.** Statistical histogram of salinity of fluid inclusions

**2.3 Composition of fluid inclusions**

The minerals (single mineral purity>98%) like garnet, magnetite, pyrite, quartz and calcite were selected, and subjected to group composition analysis on Dionex DX-120 ion chromatograph. The test results are listed in Tables 3 and 4.

It can be seen from Tables 3 and 4 that, in the liquid phase of fluid inclusions in Yueshan deposit, the main cations were Ca<sup>2+</sup>, Na<sup>+</sup>, K<sup>+</sup> and Mg<sup>2+</sup>, whose contents were 30.111~96.256×10<sup>-6</sup>, 1.406~15.729×10<sup>-6</sup>, 1.592~6.998×10<sup>-6</sup> and 7.191~11.448×10<sup>-6</sup>, respectively. The abundance of Ca<sup>2+</sup> in the metallogenic fluid is attributable to the water-rock interaction between the fluid and the carbonate. Meanwhile, the main anions include SO<sub>4</sub><sup>2-</sup> (43.981~117.831×10<sup>-6</sup>) and Cl<sup>-</sup> (5.785~37.169×10<sup>-6</sup>), plus a slight amount of F<sup>-</sup>. In the gas phase of the fluid inclusions, the content of H<sub>2</sub>O was far greater than that of any other gas phase component. In addition, the inclusions had a high presence of CO<sub>2</sub>, a certain amount of CH<sub>4</sub> and traces of C<sub>2</sub>H<sub>2</sub>, H<sub>2</sub> and C<sub>2</sub>H<sub>6</sub>.

**Table 3.** Liquid phase composition of fluid inclusions in Yueshan Cu-polymetallic deposit

ID	Object	Liquid compositions ( $10^{-6}$ )						
		F <sup>-</sup>	Cl <sup>-</sup>	SO <sub>4</sub> <sup>2-</sup>	Na <sup>+</sup>	K <sup>+</sup>	Mg <sup>2+</sup>	Ca <sup>2+</sup>
1	Garnet	3.367	15.475	117.831	4.381	-	11.448	96.256
2	Magnetite	2.763	5.785	71.260	1.406	-	-	66.000
3	Pyrite	4.513	37.169	43.981	15.729	6.998	-	39.945
4	Silica	5.345	28.682	55.707	8.309	2.049	7.197	42.837
5	Calcite	2.728	7.641	15.471	3.328	1.592	-	30.111

**Table 4.** Gas phase composition of fluid inclusions in Yueshan Cu-polymetallic deposit

ID	Object	Gas - phase components ( $10^{-6}$ )						
		H <sub>2</sub>	CH <sub>4</sub>	C <sub>2</sub> H <sub>2</sub>	CO <sub>2</sub>	C <sub>2</sub> H <sub>6</sub>	H <sub>2</sub> O	CO <sub>2</sub> /H <sub>2</sub> O
1	Garnet	1.196	17.957	-	191.874	-	932	0.206
2	Magnetite	0.597	16.591	-	116.723	-	652	0.179
3	Pyrite	2.044	28.764	-	84.299	8.124	413	0.204
4	Silica	3.289	21.468	-	214.611	-	1321	0.162
5	Calcite	0.643	6.680	-	54.775	-	933	0.059

### 3. METALLOGENIC MECHANISM

Based on the test on fluid inclusions, this chapter investigates the material, fluid and heat sources of hydrotogenesis.

#### 3.1 Material sources

##### (1) Copper and iron sources

Judging by the ore-bearing potential, the local strata contain little metallogenic materials. It is deduced that the metallogenic elements Cu and Fe of Yueshan deposit mainly come from magma, according to the geological features of the deposit and the geochemical features of the rocks. The metallogenic parent rock is the diorite-bearing Yueshan rock mass, which is closely related to metallogenesis. The target deposit lies at the front end of the rock mass. The deep mantle is the source for the original magma of the rock mass. The deep-source magma contains lots of metallogenic elements like Cu and Fe, laying the basis for the enrichment of such elements.

##### (2) Sulfur sources

The author conducted sulfur isotope tests on ores, surrounding rock and rock mass. The results show that the  $\delta^{34}\text{S}_{\text{CDT}}$  values of ores were discrete, falling in  $-11.3 \times 10^{-3} \sim +19.2 \times 10^{-3}$ . Hence, the sulfur of Yueshan mine has mainly sources, such as deep-source magma, bio-sulfur in the strata and the sulfur in the gypsum-salt layer, rather than a single source.

#### 3.2 Fluid sources

The gas-liquid phase analysis on garnet and magnetite of Yueshan mine indicates that the liquid inclusions had a high content of H<sub>2</sub>, indicating that the metallogenic fluid must come from deep source(s).

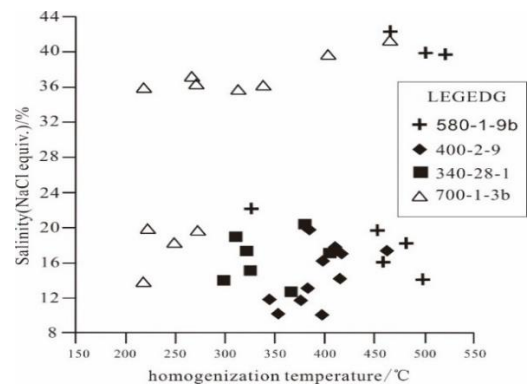
The liquid phase saw high contents of SO<sub>4</sub><sup>2-</sup>, Cl<sup>-</sup>, F<sup>-</sup>, Ca<sup>2+</sup>, Na<sup>+</sup>, K<sup>+</sup> and Mg<sup>2+</sup>. Among them, the heavy presence of Ca<sup>2+</sup> and Mg<sup>2+</sup> may be the result of the carbonate surrounding rock of Yueshan deposit. During the evolution of metallogenic fluid, the crust components must have been assimilated with the surrounding rock. The existence of Na<sup>+</sup> and Cl<sup>-</sup> in the fluid was confirmed by the small amount of salt crystals

observed under the microscope in some inclusions.

Through microscope observation and gas phase analysis, it is learned that H<sub>2</sub>O and CO<sub>2</sub> were important components in metallogenic fluid. The two components always dominated the fluid, either in gas form or liquid form, although the inclusions exhibited different features in different metallogenic stages.

#### 3.3 Heat sources

The scatterplots of homogenization temperature and salinity in liquid inclusions of Yueshan deposit are displayed in Figure 4. The two highlighted regions in the figure are the medium and high ranges of the homogenization temperature, which concentrated between 271 and 521°C.

**Figure 4.** The scatterplots of homogenization temperature and salinity in liquid inclusions of Yueshan Cu-polymetallic deposit

The mineral 580-1-9b belonged to the high temperature range of 450~521°C. The homogenization temperature of the mineral was greater than 450°C. Most of its liquid inclusions were type II, and a few were type Ia. This composition demonstrates the boiling effect of the metallogenic fluid in the early stage, when the metallogenic temperature equals the minimum temperature 450°C. This stage corresponds to the skarn stage of the skarnization hydrotogenesis period. Under the high metallogenic temperature, the main products were skarn minerals like garnet and diopside. For minerals 340-28-1 and 700-1-3b, the homogenization temperatures of their

fluid inclusions were mostly within the low to medium range of 200~320°C. Due to faulting and other tectonic activities, the hot and pressurized fluid was suddenly depressurized, resulting in boiling at reduced pressure. Thus, CO<sub>2</sub> was separated from the hot fluid. According to Williams and Ferreira (1989), CO<sub>2</sub> was originally fully mixed with the metallogenic fluid deep in the mantle; when the fluid intruded to the shallow crust, a large amount of CO<sub>2</sub> was separated from the fluid due to the plunge in solubility, leading to retrograde metamorphism and copper mineralization. This stage corresponds to the sulfide stage of the skarnization hydrothermal period through the late stage tectonic hydrothermal period. All kinds of metal sulfides were produced at this stage, and nonmetallic minerals were mainly quartz and calcite. At the same time, the fluid enriched the skarn minerals formed in the earlier stage. The Yanshanian magmatism intrusion is the major provider of both metallogenic materials and metallogenic fluid, making it the leading cause of metallogenesis in Yueshan mine. The main heat sources are the heat radiation of the ascending metallogenic fluid from the deep mantle, and exothermic reactions in the movement of metallogenic fluid.

#### 4. CONCLUSIONS

After analyzing the test results on fluid inclusions, it is concluded that the metallogenic fluid of Yueshan deposit belongs to the type of Na<sup>+</sup>+Ca<sup>2+</sup>+K<sup>+</sup>+Mg<sup>++</sup>+Cl-(SO<sub>4</sub><sup>2-</sup>), and the hot magma fluid was mineralized under 450~521°C. Yanshanian magmatic intrusion provided heat source for metallogenic hydrothermal fluid of Yueshan Cu-polymetallic deposit. The fluid activity underwent skarn hydrothermal stage and tectonic hydrothermal stage, and the skarn minerals formed in the early stage were superimposed and enriched.

#### ACKNOWLEDGMENT

This research was Funded by: the Key Scientific and Technological Research Project of Henan Province (192102310268); the Open Research Fund Program of Key Laboratory of Metallogenic Prediction of Nonferrous Metals and Geological Environment Monitoring (Central South University), Ministry of Education(2019YSJS08) and the Nanhu Scholars Program for Young Scholars of XYNU; the special projects for promoting the development of big data of Guizhou Institute of Technology; the Geological Resources and Geological Engineering, Guizhou Provincial Key Disciplines, China (ZDXK [2018]001).

#### REFERENCES

[1] Liu, L.M., Wan, C.L., Zhao, C.B., Zhao, Y.L. (2011). Geodynamic constraints on orebody localization in the Anqing Orefield, China: Computational modeling and facilitating predictive exploration of deep deposits. *Ore Geology Reviews*, 43(1): 249-263. <https://doi.org/10.1016/j.oregeorev.2011.09.005>

[2] Yang, G.S., Yan, Y.F., Feng, P.Y. (2013). Ore-forming fluid system of the Anqing Cu-Fe deposit, Anhui Province, China. *Advanced Materials Research*, 734-737: 135-138.

<https://doi.org/10.4028/www.scientific.net/AMR.734-737.135>

[3] Yang, G. (2015). Magmatic-fluid-metallogenic system of the Anqing skarn Cu-Fe deposit, Anhui province, China. *Acta Geologica Sinica*, 88(s2): 1705-1707. [https://doi.org/10.1111/1755-6724.12385\\_52](https://doi.org/10.1111/1755-6724.12385_52)

[4] Gu, H., Duan, L., Yang, X. (2015). Zircon U-Pb geochronology and Hf isotopic geochemistry of the Liwan Cu-Mo deposit, Guichi ore cluster field. *Acta Geologica Sinica*, 88(s2): 1607-1608. [https://doi.org/10.1111/1755-6724.12385\\_7](https://doi.org/10.1111/1755-6724.12385_7)

[5] Duan, L.A., Gu, H.L., Yang, X.Y., Yan, Z.Z. (2015). Chronology and Hf isotopic study of igneous rocks in the Liwan Cu-polymetal deposit in Guichi along the Middle-Lower Yangtze River. *Acta Petrologica Sinica*, 31(7): 1943-1961.

[6] Duan, L.A., Gu, H.L., Yang, X.Y. (2017). Geological and geochemical constraints on the newly discovered Yangchongli gold deposit in Tongling region, lower Yangtze metallogenic belt. *Acta Geologica Sinica*, 91(6): 2078-2108. <https://doi.org/10.3969/j.issn.1000-9515.2017.06.009>

[7] Liu, Z.F., Shao, Y.J., Shu, Z.M., Peng, N.H., Xie, Y.L., Zhang, Y. (2012). Fluid inclusion characteristics of Longmenshan copper-polymetallic deposit in Yueshan, Anhui Province, China. *Journal of Central South University*, 19(9): 2627-2633. <https://doi.org/10.1007/s11771-012-1320-y>

[8] Zhou, T.F., Yu, F., Feng, Y., Zhang, L.J., Qian, B., Ma, L., Yang, X.F., David, R.C. (2011). Geochronology and significance of volcanic rocks in the Ning-Wu Basin of China. *Science China Earth Sciences*, 54(2): 185-196. <https://doi.org/10.1007/s11430-010-4150-5>

[9] Brown, P.E. (1989). FLINCOR: A microcomputer program for the reduction and investigation of fluid inclusion data. *American Mineralogist*, 74: 1390-1393.

[10] Serttikul, C., Datta, A.K., Rattanadecho, P. (2019). Effect of layer arrangement on 2-D numerical analysis of freezing process in double layer porous packed bed, *International Journal of Heat and Technology*, 37(1): 273-284. <https://doi.org/10.18280/ijht.370133>

[11] Wei, Y., Wang, L., Yang, G.S. (2018). Temperature field distribution of a freeze sinking shaft under seepage conditions in cretaceous formation of Western China, *International Journal of Heat and Technology*, 36(3): 1055-1060. <https://doi.org/10.18280/ijht.360336>

[12] Abourabia, A.M., Abdel, Moneim, S.A. (2019). Analytical solution of sea water steady magneto-hydrodynamic equations subjected to stretching sheet under induced magnetic field and heat transfer, *Mathematical Modelling of Engineering Problems*, 6(1): 141-151. <https://doi.org/10.18280/mmep.060119>

[13] Ike, C.C. (2018). Energy formulation for flexural – torsional buckling of thin-walled column with open cross- section, *Mathematical Modelling of Engineering Problems*, 5(2): 58-66. <https://doi.org/10.18280/mmep.050202>

[14] Brown, P.E., Lamb, W. (1989). M.P-V-T properties of fluids in the system H<sub>2</sub>O-CO<sub>2</sub>-NaCl: New graphical presentations and implications for fluid inclusion studies. *Geochimica et Cosmochimica Acta*, 53(6): 1209-1221. [http://doi.org/10.1016/0016-7037\(89\)90057-4](http://doi.org/10.1016/0016-7037(89)90057-4)